

Performance Measurement of 802.11a Wireless Links from UAV to Ground Nodes with Various Antenna Orientations

Chen-Mou Cheng Pai-Hsiang Hsiao H. T. Kung Dario Vlah
{doug, shawn, htk, dario}@eecs.harvard.edu
Division of Engineering and Applied Sciences
Harvard University
Cambridge, MA 02138

ABSTRACT

We report measured performance of 802.11a wireless links from an unmanned aerial vehicle (UAV) to ground stations. In a set of field experiments, we record the received signal strength indicator (RSSI) and measure the raw link-layer throughput for various antenna orientations, communication distances and ground-station elevations. By comparing the performance of 32 simultaneous pairs of UAV and ground station configurations, we are able to conclude that, in order to achieve the highest throughput under a typical flyover UAV flight path, both the UAV and the ground station should use omni-directional dipole (as opposed to high-gain, narrow-beam) antennas positioned horizontally, with their respective antenna null pointing to a direction perpendicular to the UAV's flight path. In addition, a moderate amount of elevation of the ground stations can also improve performance significantly.

I. INTRODUCTION

We envision that in the future, low-flying UAVs could provide a cost-effective wireless networking means for ground devices. Such UAV-based wireless networking could have a number of advantages, including (1) that UAVs can provide on-demand, high-quality communication due to line-of-sight signal propagation; (2) that UAVs can be sensing and data-fusion nodes dynamically deployable in the region of interest; (3) that UAVs can tailor their flight paths to enhance the quality of wireless networking and communication; and, finally, (4) that UAVs can themselves carry and forward huge amounts of data, e.g., gigabytes of terrain images or databases. With these capabilities, a UAV-based network can, for example, provide high-speed transport of multimedia data (e.g., videos and images) for ground nodes and overcome environmental shadowing effects caused by blocking structures such as mountains and tall buildings.

The UAV-based networking approach has become especially attractive in the recent years due to the availability of low-cost,

This material is based on research sponsored by Air Force Research Laboratory under agreement numbers FA8750-05-1-0035 and FA8750-06-2-0154. The U.S. Government is authorized to reproduce and distribute reprints for Governmental purposes notwithstanding any copyright annotation thereon. The views and conclusions contained herein are those of the author and should not be interpreted as necessarily representing the official policies, either expressed or implied, of Air Force Research Laboratory or the U.S. Government.

Commercial Off-The-Shelf (COTS) wireless equipment, such as IEEE 802.11 wireless LAN ("WiFi") [4]. For example, by integrating compact, 802.11 wireless equipment into a small 94-inch wing-span UAV, we can readily create a powerful networking node in the air [8].

In this paper, we address the issue of configuring 802.11 antennas in UAV-based networking. It is well-known that antenna types (e.g., omni or directional) as well as their positions and orientations can greatly affect the performance of wireless links [2], [3]. In addition, when a UAV communicates with ground nodes, we need to consider ground effects (such as interference from reflected signals, modeled by two-ray propagation [6]). Given the large number of complicated issues involved, it is essential that we conduct field experiments in order to understand the performance impact of various antenna configurations at the application level.

We have instrumented a UAV and several ground nodes with two types of 802.11a antennas in various orientations. Using this equipment, we have conducted a set of flight tests to measure their raw link-layer throughput performance in the field. In this paper, we report and analyze our findings from these flight tests (Sections II, III). Furthermore, we report the measured received power as a function of communication distance and their correlation (Section IV). These results provide baseline performance information on 802.11a wireless links for UAV and ground node communication. They can be useful for future work in UAV networking, such as antenna selection strategies and multi-hop wireless networking.

II. FIELD EXPERIMENT SETUP

Our networking testbed consists of a UAV node and several ground nodes, all equipped with 802.11a wireless devices. The ground nodes were placed on a line, with about 6 ft separation between the two end nodes. For these nodes, we used two types of single-board computers, made by Thecus and Soekris. Our UAV is based on the Senior Telemaster model [7]. We conducted our flight experiments at a private airfield in Woodstock, Connecticut. In these experiments, we used Atheros-chipset-based Wistron CM9 802.11a/b/g adapters, with 18dBm transmit power and channel 56 in the 802.11a band.

We encountered a serious problem where our single-board computer would interfere with the 72MHz R/C receiver on the airplane, possibly due to noise from the 66MHz system bus.

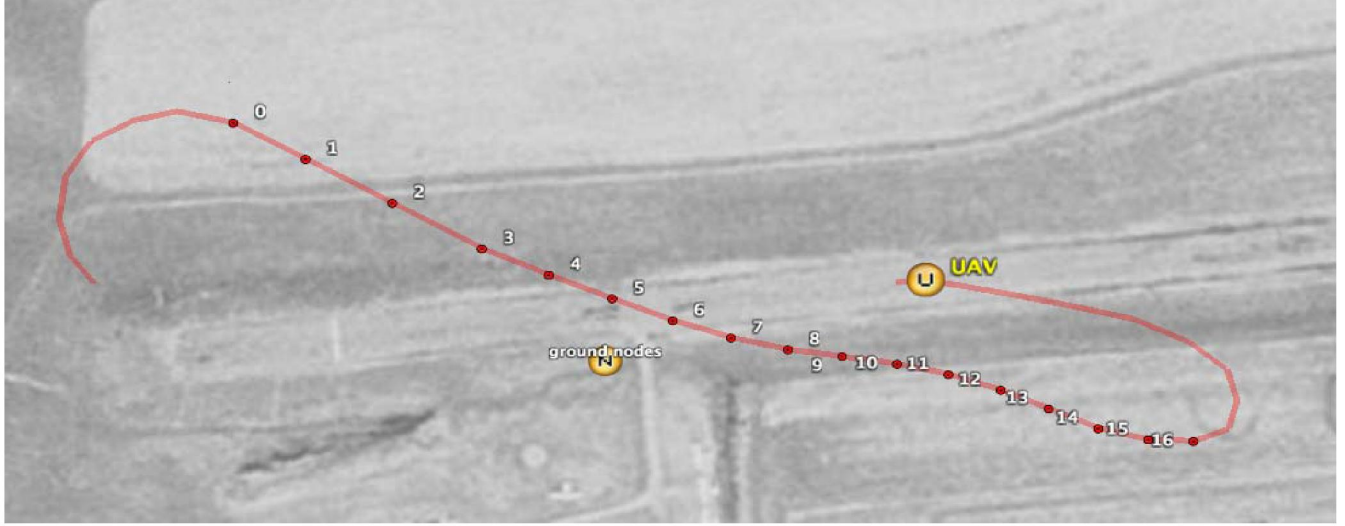


Fig. 1. A U.S. Geological Survey (USGS) satellite map showing the location of an elevated ground node (N), node 3 in Figure 5, and a sample UAV path in a fly test. The horizontal, light-colored band under the UAV node (U) is the airport runway, which is approximately 25 yards wide. The dots show the positions reported by the GPS once a second.

We solved the interference problem by doing three things: (1) moving the R/C receiver to the back of the airplane, (2) shielding the box hosting the single-board computer with metal screen wrap, and (3) moving the computer on/off switch and its wire—which was radiating the board noise—into the shielded enclosure.

We used two types of antennas on both the UAV and ground nodes. One was a 7-dBi, 2.4/5 GHz dual-band, omni-directional antenna purchased from a commercial vendor (Netgate), and the other was a custom 2-dBi dipole antenna. Samples of these antennas are shown in Figure 2. The key difference between these two antenna types is that the Netgate antenna produces an omni-directional beam that is much narrower in the vertical direction than the dipole, as can be seen from the manufacturer’s radiation pattern plot in Figure 3.

The UAV was equipped with two wireless adapters, each with two antennas. The UAV would broadcast data packets using its four antennas in a round-robin manner. Each ground node was equipped with two wireless adapters, each with one antenna. Both adapters of a ground node could simultaneously receive UAV’s packets. One of the four ground nodes was mounted on the top of a 14-ft wooden pole. Later in this section we will describe the antenna configurations and traffic patterns in detail.

The UAV flew approximately at 50-yard altitude and at 40 miles per hour over the ground nodes. The UAV had an on-board GlobalSat BU-353 GPS receiver, which provided position information at 1 second intervals. The GPS readings allowed us to visualize in real time, on a laptop, the UAV moving on a U.S. Geological Survey (USGS) satellite map shown in Figure 1. We have performed a coarse calibration of the GPS; our estimate of the position error was about 5 meters. The UAV GPS trace and the static ground node coordinates allowed us to analyze various performance parameters as

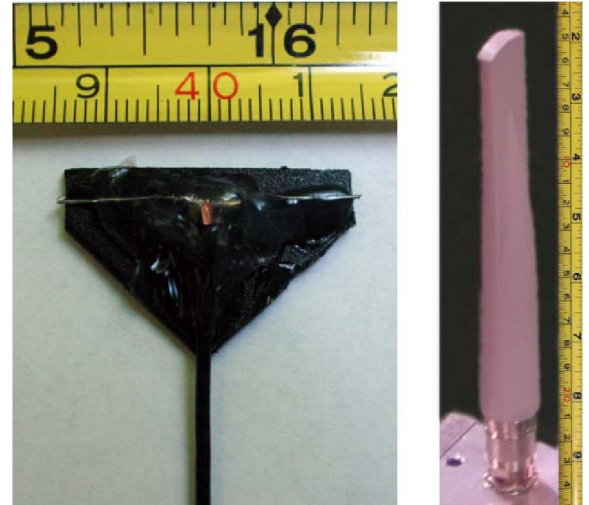


Fig. 2. Samples of the two antenna types used in our testbed. Left: our hand-made dipole antenna, tuned to 5.28 GHz (channel 56). Right: the off-the-shelf Netgate antenna.

functions of distance.

A. Antenna Configurations

The antennas were configured as follows. First, let us define the following labels for referring to various antenna types and orientations:

H	horizontal dipole (i.e., dipole is parallel to the ground), orthogonal to flight direction
H_N	horizontal Netgate antenna, orthogonal to flight direction
H_p	horizontal dipole, parallel to flight direction
V	vertical dipole (i.e., dipole is perpendicular to the ground)
V_N	vertical Netgate antenna

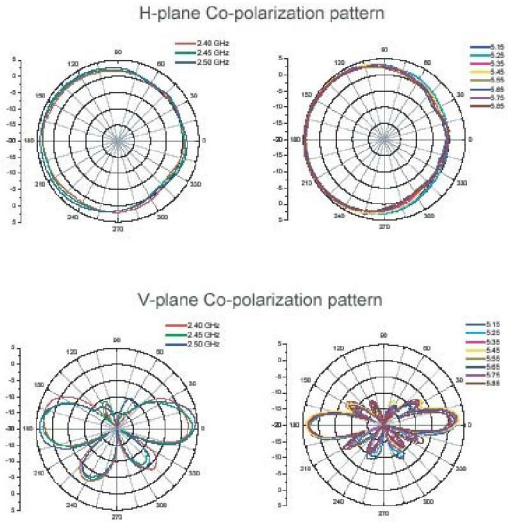


Fig. 3. The radiation pattern of the Netgate antennas.

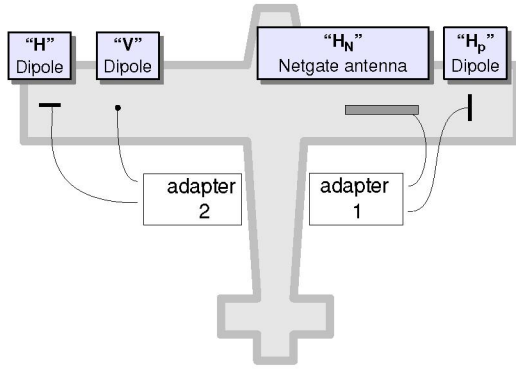


Fig. 4. The UAV antenna setup.

The UAV carried 4 antennas, H_p , H_N , H , and V , as depicted in Figure 4. The ground nodes each carried two antennas—one on each wireless adapter. The following table lists their antenna orientations, derived relative to a straight flight path along the direction of the runway:

	Node 1	Node 3	Node 5	Node 6
Antenna 0	V	H	H	H_p
Antenna 1	H	V_N	V_N	V_N

Figure 5 depicts the flight pattern of the UAV and the orientations of the ground antennas.

B. Description of Traffic Patterns

The UAV was the sole data transmitter during the experiment. It generated an endless stream of sequenced 320-byte UDP packets (which means roughly a $500 \mu\text{s}$ packet transmission time at the 6Mbps rate) and broadcast them over its 4 antennas in an approximately round-robin order. More specifically, a user-mode program alternated enqueueing

pairs of packets into the first and second network adapter's socket queue; the kernel-level driver would add a timestamp and output each packet to the antenna identified by the least significant bit of the sequence number. For example, of the first 4 packets, numbered 0-3, packets 0 and 1 would go to the first adapter, while 2 and 3 would go to the second. Furthermore, packets 0 and 2 would be sent using each adapter's first antenna, while 1 and 3 would go out on the second antennas.

One reason for such a multiplexing scheme is to avoid interference between probe packets; in this scheme, the packets are interleaved in time so that at any moment, there is at most one packet in the air. It is for the same reason that we decided in the experiment to have the UAV node as the sole transmitter and evaluate only the performance of one-way communication from UAV to the ground. Full bidirectional measurements would otherwise require scheduled transmissions from ground nodes, which would lead to unacceptably large guard times and thus significantly decrease the temporal resolution of the measurement. Fortunately, under the typical symmetric-link assumption in free-space or nearly free-space propagation models, these unidirectional link measurements can still be useful in characterizing the bidirectional UAV-ground links.

Under this multiplexing scheme, ideally each antenna would send one packet every 2ms. Indeed, individual transmit queues always contain packets for alternating antennas; however, the combined output of the two adapters can not be perfectly interleaved since the sending pattern is subject to the random backoff in the 802.11 CSMA mechanism. We measured the resulting interleaving pattern in the lab, and found that runs of packets from the same adapter had at most 7 packets, while their mean length was 1.53 packets.

The ground nodes captured the broadcast packets using two wireless adapters and recorded the transmit timestamp, sequence number, size, and the RSSI figure. This way, from the data traces of just one ground node we can obtain the performance for the 8 different links created by the combination of 4 UAV and 2 ground node antennas. Therefore, the combined traces of all 4 ground nodes contain the performance for 32 different antenna combinations.

The reason for measuring so many link combinations nearly simultaneously is to eliminate the variations that would in-

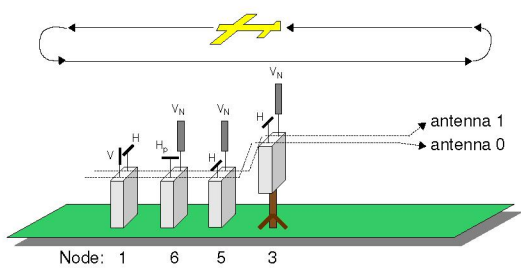


Fig. 5. Orientations of the antennas on the ground nodes relative to the UAV flight pattern. The thick gray sticks represent Netgate antennas.

evitably occur if we measured the different links using separate UAV flights. All of our 32 traces contain data points that lie at most several milliseconds apart, which is short enough to regard many physical parameters of the environment constant. For example, it may take several hundreds of milliseconds for the bank angle of the UAV to change enough to appreciably affect the receiver's position in the antenna pattern. This is also long enough that we can fairly compare many interesting properties for the 32 links, such as throughput, signal strength and packet loss.

III. MEASURED THROUGHPUT AS A FUNCTION OF ANTENNA ORIENTATION

In this section, we report the throughput measurement results, based on which we compare the performance of several different antenna configurations and identify the best one.

As described in Section II, in the experiments, the UAV node was constantly sending out UDP packets at 6Mbps, or 1.5Mbps from each of the four transmit antennas. By counting the number of received packets at a receive antenna in a short period of time, we can measure the instantaneous performance of that particular antenna orientation configuration, which we will call "the UDP throughput." We use this throughput as the main performance metric in evaluating various antenna orientation configurations.

The total flight time in the two flights reported is approximately 24 minutes, during which the UAV node sent out more than 2.4 million packets. The total number of packets received at the eight antennas of the four ground nodes is about 1.8 million; however, most of the packets are received by more than one antenna, and therefore, the achieved end-to-end throughput, averaged over all antennas, is merely 120.8 kbps. Due to the relatively large flight area, the UAV node and the ground nodes are out of each other's communication range for a significant portion of time. For this reason, out of all possible antenna orientation configurations, even the best configuration (horizontal transmit antenna to elevated horizontal receive antenna) only receives about 33% of the packets. We plot the UDP throughput of the top four best-performing antenna configurations versus distance in Figure 6.

There are four curves in Figure 6. Following the order described in the legend, the topmost curve represents the throughput achieved from a horizontally oriented dipole antenna on the UAV node to another horizontally oriented dipole antenna on an elevated ground node; this combination is the best antenna orientation configuration we have seen in this experiment. The second topmost one differs from the previous one in that the ground node is not elevated. By comparing the two, we can see that an elevation of 14 feet helps achieve a significantly higher throughput. The third curve shows the throughput from a vertically oriented dipole antenna on the UAV node to another vertically oriented dipole antenna on a ground node. It is interesting to note that, although inferior to other three configurations when the distance is small, this configuration actually outperforms the two horizontal configurations in which the ground node is not elevated when the

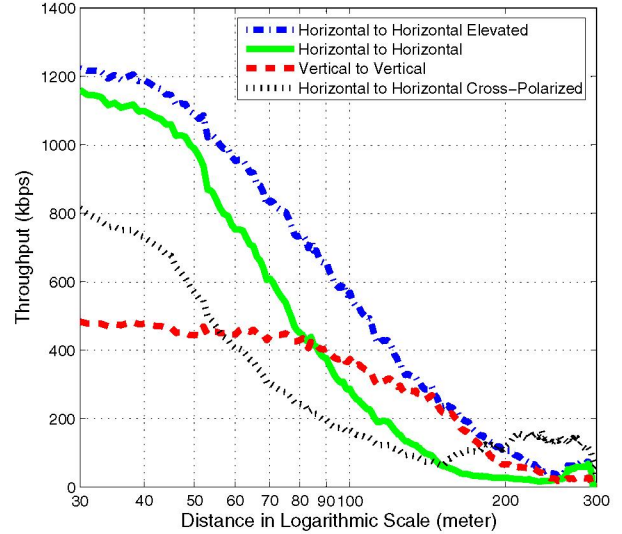


Fig. 6. The UDP throughput of the top four best-performing antenna configurations.

distance is large enough. This is because when the distance is small, the vertically oriented dipole antennas on the transmitter and the receiver are more likely to be in each other's null, resulting in worse performance, whereas it is less likely for the two antennas to be in each other's null when the distance is large. Lastly, the bottom curve corresponds to a pair of cross-polarized dipole antennas on the UAV node and a ground node. To our surprise, this configuration actually performs quite well, especially at the farthest distance of around 300 meters. We believe that this is because when the UAV is at that distance, it is probably banking at sharp angles such that it turns back towards the ground nodes; at this time, the antennas are no longer cross-polarized. We have looked more closely into the GPS trace and found that the furthest distance between the UAV and the ground nodes during the entire course of the flight is around 300 to 350 meters, further confirming our theory.

We summarize the best throughput results for various antenna orientation configurations in Table I. Overall, the horizontal/horizontal antenna orientation configuration has the best performance; furthermore, elevating the ground node can also help improve throughput. Cross-polarization in general has a negative impact on performance; this is evident from the vertical/horizontal combinations in Table I. Finally, we find that the off-the-shelf Netgate antennas perform poorly compared with dipole antennas, most likely due to their narrow beams along the vertical direction.

IV. MEASURED RECEIVED POWER AS A FUNCTION OF DISTANCE

In this section, we investigate the correlation between measured received power and distance. In particular, we perform linear regression on received power and distance following a

Transmit Antenna	Receive Antenna	Throughput
H	H Elevated	433 kbps
H	H	289 kbps
V	V	246 kbps
H_p	H Elevated	223 kbps
V	H Elevated	160 kbps
H_p	H	143 kbps
V	H_p	137 kbps
H_p	V	119 kbps
V	V_N	110 kbps

TABLE I

The throughput performance of various antenna orientation configurations.

log-distance path loss model. The correlation coefficient of the linear regression can tell us whether there is a correlation between received power and distance. We are also interested in the slope of the linear regression, because it gives us the path loss exponent of the environment.

Under the log-distance path loss model, received power (measured in dBm) is expressed as a function of the logarithm of distance. More specifically, the received power $P_r(d)$ at distance d can be computed from received power $P_r(d_0)$ at distance d_0 with the following formula (α being the path loss exponent):

$$P_r(d) = P_r(d_0) - 10\alpha \log_{10}\left(\frac{d}{d_0}\right) \quad (1)$$

For each packet received by the ground nodes, we logged its RSSI as reported by the Atheros cards. We then derived the received power for each packet from the reported RSSI. It has been shown that there is a constant difference of -95 between the RSSI and the actual received power when RSSI is greater than 6 [9]. Based on that finding, we derived received power (in dBm) by adding -95 to the reported RSSI.

We recorded GPS readings on the UAV node and on the elevated ground node (node 3 in Figure 5) to derive distance between the two nodes. Because the GPS only reports coordinate every second, we need to estimate the coordinate of the UAV when a packet is being transmitted. We estimated the coordinate by performing linear interpolation between two enclosing GPS reports and use it to compute distance.

As input to the correlation computation we use data from the 17 second flyover segment depicted in Figure 1. We chose this particular segment because its path is close to a straight line, so the variations in relative antenna orientations due to UAV turning and banking are expected to be small.

Figure 7 shows the correlation of the measured received power and distance during this flyover; each red marker represents one packet. The packets plotted are those transmitted from the UAV H antenna and received by the H antenna of Node 3 (the elevated node). We chose this particular antenna pair because the distance—not randomness induced by, e.g., ground reflection—should be the dominating effect on the receive power due to elevation. The straight line in the

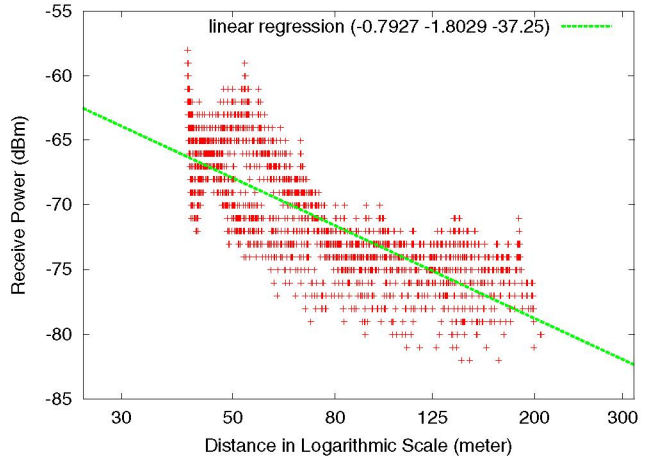


Fig. 7. Received power vs. distance and linear regression result for the flyover shown in Figure 1. Each marker represents a packet, and the numbers in the parentheses are correlation coefficient, slope, and intercept.

figure represents the output of linear regression. Specifically, the correlation coefficient is -0.7927 , slope -1.8029 , and intercept -37.25 .

The correlation coefficient indicates there is a good correlation between received power and distance. However, the absolute value of the slope, which can be interpreted as the path loss exponent, is lower than expected: for this experiment, we expected α to be greater than 2 , but the slope of -1.8029 suggests a path loss exponent less than 2 .

We believe that such low path loss exponent can be explained by the limitation of our 802.11 equipment and the dynamic range of the received power in this experiment. More specifically, when the received power of a packet is too low, the equipment can not decode it; as a result, no RSSI is reported for that particular packet. As the distance increases, there will be more packets that can not be decoded due to low RSSI. This causes the distribution of received power vs. distance to be skewed when the distance is large. That is, at long distance only packets of sufficiently high received power are recorded, while packets of low received power are dropped. As a result, absence of packets of low received power results in a skewed regression slope.

To better measure the correlation of received power and distance, we would need to revise our experimental setup. We would need to raise the operating received power range of our experiments so the distribution of receive power are not distorted at long distance. We would also want to repeat the experiments using 802.11b/g in order to obtain measurements of wider range of distance.

V. DISCUSSION

In Section III we reported throughput measurements based on data taken during 24 minutes of UAV flights. We now take a closer look at the flyover segment depicted in Figure 1, in order to study transmission performance apart from the various

other segments where the UAV motion is not as regular. Furthermore, we narrow down the data set to that received by antenna H of the elevated ground node (node 3), since it would be the least affected by ground effects.

Table II lists the throughputs achieved during the flyover from the four UAV antennas. The performance of antenna pairs orthogonal to the flight path ($H-H$ and H_N-H) is noticeably better than the other two; even the second-best pair performs more than twice as well as the third-best. On the other hand, the worst performer is the $V-H$ pair, possibly due to cross-polarization and the fact that the receiver is placed closer to the antenna null region of the transmitter.

H	0.63101 Mbps	(42.1%)
H_N	0.59425 Mbps	(39.6%)
V	0.23607 Mbps	(15.7%)
H_p	0.16682 Mbps	(11.1%)

TABLE II

The throughput performance of four UAV antennas to the H antenna on the elevated ground node, expressed in megabits per second and as fractions of the maximum possible throughput.

Figure 8 shows the raw RSSI data from the flyover. This data agrees with the throughput measurements in that the strongest signal comes from the H and H_N antennas. Furthermore, the plots uncover two additional observations.

First, we note that even though its performance is second best, the H_N antenna exhibits a significant peak around 10s into the flyover. This is not an isolated incident, since we observed similar peaks on other flyover traces. We believe that this is caused by the H_N antenna's narrow beam pattern—as the UAV flies and banks at varying angles toward the ground nodes, it occasionally “hits” them with the main lobe of the H_N antenna. The narrow beam seems to be a disadvantage here, since it increases the variation in link quality without actually beating the wide-beam antenna in throughput performance.

The second observation is that the signal strength of the best antenna pair does not vary smoothly as the UAV flies over the ground nodes; instead, we can see at least three major peaks in the curve for antenna H . Since the antennas in this pair have axially symmetric beam patterns, the peaks cannot be explained by the UAV motion alone. Instead, we believe that the cause is interference from a reflected ray as modeled by two-ray propagation.

Some receiving antennas, other than those in Figure 8, performed very poorly. For example, the V_N antenna of Node 5 did not receive any packets at all. It turns out that most poor performers were V_N antennas; we believe that their narrow horizontal beam patterns were largely underneath the UAV. This further illustrates the difficulty with use of directional antennas.

VI. CONCLUSIONS

Our measurement data have shown that, for UAV’s communication with a ground node, horizontal dipole antennas with

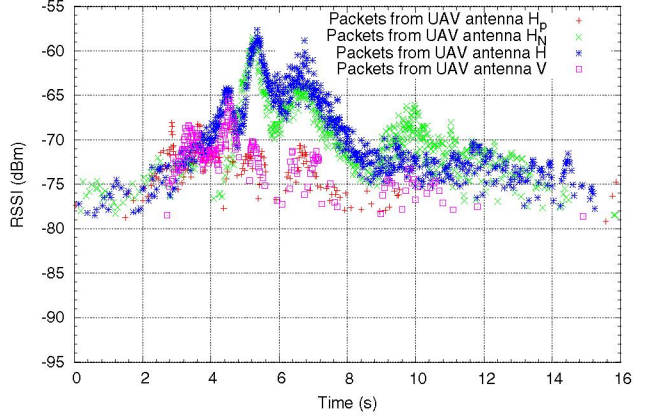


Fig. 8. There are four sets of points shown, corresponding to packets coming from each of the UAV’s four antennas.

their nulls pointing to a direction perpendicular to the UAV flight path yields the highest throughput among 32 antenna pair configurations. In addition, the measurement data suggest that the path loss in an airfield environment is roughly proportional to the square of the communicating distance. These results appear to be among the first antenna measurement results for 802.11 based UAV networking. We chose to start our measurement work with 802.11a because there is relatively less interference from the environment in the 5GHz band. We plan to conduct similar measurements for 802.11 b/g in the future.

REFERENCES

- [1] Li, J., Blake, C., De Couto, D. S. J., Lee, H. I., and Morris, R., “Capacity of Ad Hoc Wireless Networks,” *ACM MobiCom*, July 2001
- [2] Aguayo, D., Bicket, J., Biswas, S., Judd, G., and Morris, R., “Link-level Measurements from an 802.11b Mesh Network,” *SIGCOMM 2004*, Aug 2004
- [3] Bicket, J., Aguayo, D., Biswas, S., and Morris, R., “Architecture and Evaluation of an Unplanned 802.11b Mesh Network,” *ACM MobiCom 2005*, Aug 2005
- [4] IEEE 802.11 Working Group, “Wireless LAN Medium Access Control (MAC) and Physical Layer (PHY) specifications,” *IEEE 802.11 standard, including 802.11a and 802.11b extensions*, Sep 1999
- [5] Haykin, S., “Communication Systems,” *John Wiley & Sons, Inc.*, 2001.
- [6] Lee, W. C. Y., “Mobile Communications Engineering: Theory And Applications,” *McGraw Hill*, 1997.
- [7] Hobby Lobby International, Inc., “Senior Telemaster R/C Airplane,” <http://www.hobby-lobby.com/srtele.htm>, 2006.
- [8] Brown, T. X., Argrow, B., Dixon, C., et al., “Ad Hoc UAV Ground Network (AUGNet),” *AIAA 3rd “Unmanned Unlimited” Technical Conference*, Chicago, IL, 2004
- [9] Judd, G., and Steenkiste, P., “A Simple Mechanism for Capturing and Replaying Wireless Channels,” *E-WIND ’05: Proceeding of the 2005 ACM SIGCOMM workshop on Experimental approaches to wireless network design and analysis*, 2005